


Sound attenuation in two-dimensional glasses at finite temperatures

Licun Fu and Lijin Wang*

School of Physics and Optoelectronic Engineering, Anhui University, Hefei 230601, China
 (Received 28 July 2022; revised 27 September 2022; accepted 24 October 2022; published 10 November 2022)

The thermal conductivity of glasses exhibits an unusual temperature dependence compared to their crystalline counterparts. Sound attenuation due to disorder in glasses was proposed to be important in rationalizing this special behavior. Simulation studies suggest that in the harmonic approximation, the sound attenuation follows Rayleigh scattering scaling at small wave vector in both two-dimensional (2D) and 3D glasses. The influence of the anharmonicity on sound attenuation has very recently been investigated numerically, but only in 3D glasses. Hence, it remains unknown in simulations how sound attenuation changes with the wave vector in 2D glasses when the anharmonicity comes into play. Here, we address this issue by performing computer simulations in low-temperature 2D glasses over a large range of glass stabilities. We find that the way the anharmonicity affects sound attenuation in 2D glasses is the same as that in 3D, thus revealing that numerically the influence of the anharmonicity on sound attenuation does not rely on the spatial dimension.

DOI: [10.1103/PhysRevE.106.054605](https://doi.org/10.1103/PhysRevE.106.054605)

I. INTRODUCTION

Different from ordered crystals, glasses are well known to be characteristic of disorder in structures or other physical observables [1,2]. The intrinsic disorder endows glasses with various thermal and vibrational properties [3–9] that are markedly different from their crystalline counterparts. One is that the thermal conductivity κ in glasses exhibits an unusual temperature T dependence. Specifically, κ below around 1 K behaves as T^2 in glasses, instead of T^3 as observed in crystals. Moreover, near approximately 10 K, κ exhibits a T -independent plateau, which is different from how κ performs in crystals within the same temperature regime. Such abnormal behavior in the thermal conductivity has been suggested to originate potentially from sound attenuation of glasses due to the disorder, which also constitutes one important reason to study sound attenuation in glasses.

In the literature, one could find that sound attenuation in glasses has been a subject of persistent research up to now. Although there have been some theoretical explanations or predictions with respect to sound attenuation under different theoretical frameworks [11–15], the physical origin of it seems to still be debated. Moreover, there even seems to be no consensus on how sound waves are attenuated in simulation studies of different glasses. Some simulation studies [16–19] have demonstrated that in the harmonic approximation, sound attenuation Γ follows Rayleigh scattering scaling at small wave vectors k in two-dimensional (2D) and 3D glasses, i.e., $\Gamma \sim k^{d+1}$ with d spatial dimension, while $\Gamma \sim k^2$ at large k , independent of d . In between the small- k $\Gamma \sim k^{d+1}$ and the large- k $\Gamma \sim k^2$ regimes, it was suggested in Ref. [20] that there is a logarithmic correction to the Rayleigh scattering scaling regime, i.e., $\Gamma \sim k^{d+1} \ln(k)$. However, this logarithmic behavior was subsequently demonstrated to be nearly absent

in very stable glasses [16]. In addition, there have been studies [21] suggesting that Γ exhibits a linear relation with k at higher k beyond the high- k quadratic scaling region.

Moreover, there seems to be a more complex picture with respect to sound attenuation in realistic low-temperature glasses, where anharmonic effects induced by, e.g., thermal motions, may come into play. The anharmonicity caused by thermal motions is suppressed and negligible at very low temperatures, but becomes gradually obvious with the increase of temperature. In scattering experiments [22–25] where anharmonicity is non-negligible, it was suggested that $\Gamma \sim k^2$ in small- and large- k regimes, with the Rayleigh scattering scaling in between. However, it was also observed that $\Gamma \sim k$ instead of $\Gamma \sim k^2$ at small wave vector in one experimental study of vitreous germanium [26].

The influence of the anharmonicity on sound attenuation has very recently been investigated by simulations, but only in 3D glasses. Simulation studies [27,28] of low-temperature monodisperse Leonard-Jones 3D glasses found that $\Gamma \sim k^{1.5}$ at small wave vector, with the Rayleigh scattering and $\Gamma \sim k^2$ scalings in the intermediate- k and large- k regimes, respectively. Wang *et al.* [29] examined the sound attenuation in low-temperature polydisperse inverse-power-law-potential 3D glasses over a wide range of glass stabilities. They found $\Gamma \sim k^{1.5}$ for an ageing glass, which is easily observed in poorly annealed glass, while $\Gamma \sim k^2$ when there is no ageing on the calculated timescale. The nonquadratic scaling of Γ is consistent with the prediction of fluctuating elasticity theory [11,26,30]. This theory predicts that the anharmonicity results in a nonquadratic scaling of Γ in glasses which are on the verge of an elasticity instability, but a quadratic scaling in glasses far away from the instability. However, there seems to be no direct evidence showing that those glasses showing nonquadratic scaling of sound attenuation studied by Wang and co-workers [29], and Mizuno and co-workers [27,28], are close to an elasticity instability. A compilation of studies in 3D glasses could reach one common conclusion that the

*lijin.wang@ahu.edu.cn

anharmonicity mainly affects the behavior of the small-wave-vector sound attenuation [27–29].

Interestingly, the sound attenuation was suggested to be correlated to the low-frequency vibrational modes in excess of Debye prediction in both 2D and 3D glasses [10,16,18,31]. Very recently, it was demonstrated explicitly in Ref. [31] that these excess modes' density scales differently in 2D glasses than in 3D glasses, which further implies that the properties of glasses and glass-forming liquids may not be extrapolated across different spatial dimensions [32]. This also motivates us to check numerically whether the effect of anharmonicity on sound attenuation depends on the spatial dimension.

In this work, we studied low-temperature sound attenuation in 2D glasses over a wide range of stabilities, from very poorly annealed to very stable glasses with stability comparable to experimental glasses. When the anharmonicity induced by temperature comes into play, in all glasses examined, we observe $\Gamma \sim k^\beta$ with $\beta \neq 3$ at very low wave vector. Specifically, for poorly annealed glasses, we find β varies from 1.5 to 2.0 with waiting times increased, while for very stable glasses, we can always observe $\beta = 2.0$ within our available range of waiting times. Our main conclusions in 2D glasses are almost the same as those observed in 3D glasses [29]. Hence, our findings suggest that the anharmonicity effect on the low-frequency (low-wave-vector) sound attenuation does not depend on spatial dimension.

II. SIMULATION DETAILS

We simulated a continuous polydisperse two-dimensional system composed of $N = 20\,000$ particles with equal mass $m = 1$. The number density is $\rho = 1.0$. Periodic boundary conditions are applied in both two directions. The interaction between particles i and j is the purely repulsive inverse power-law potential, $V(r_{ij}) = (\frac{\sigma_{ij}}{r_{ij}})^{12} + c_0 + c_1(\frac{r_{ij}}{\sigma_{ij}})^2 + c_2(\frac{r_{ij}}{\sigma_{ij}})^4$, when their separation r_{ij} is smaller than the cutoff distance $r_{\text{cut}} = 1.25\sigma_{ij}$, and zero otherwise. Here, the constants c_0 , c_1 , and c_2 are set to guarantee the continuity of the potential at r_{cut} up to its second derivative. The distribution of the particle diameter σ follows $p(\sigma) \sim \sigma^{-3}$, and we determine the cross diameter between particles i and j through the nonadditive mixing rule, i.e., $\sigma_{ij} = \frac{\sigma_i + \sigma_j}{2}(1 - 0.2|\sigma_i - \sigma_j|)$. Details regarding our simulation model could also be found in Ref. [33].

We employed the swap Monte Carlo method [34] to prepare equilibrated supercooled liquids at different parent temperature T_p , which ranges from $T_p = 0.40 > T_{\text{onset}}$ down to $T_p = 0.03 < T_g$; here, $T_{\text{onset}} \approx 0.25$ is the onset temperature of slow dynamics and $T_g \approx 0.082$ is the estimated experimental glass transition temperature [33]. We performed molecular dynamics simulations using the LAMMPS program package [35,36] to obtain finite-temperature glasses. First, we created a zero-temperature ($T = 0$) glass by performing an instantaneous quench of a configuration equilibrated at T_p down to zero temperature, and the energy minimization method used is the conjugate gradient algorithm. Second, we heated the $T = 0$ glass to the desired T in the NVT ensemble. Third, the resulting glass was equilibrated for a time of t_w , which is in the following referred to as waiting time. Finally,

we collected data in the NVE ensemble. The average was taken over 40 different initial configurations equilibrated at T_p .

Following the previous procedure [29] to get sound attenuation information, we calculate the transverse (T) and longitudinal (L) current density correlation functions, which read

$$C_\lambda(k, t) = \left\langle \frac{\vec{J}_\lambda(k, t) \cdot \vec{J}_\lambda(-k, 0)}{\vec{J}_\lambda(k, 0) \cdot \vec{J}_\lambda(-k, 0)} \right\rangle, \quad (1)$$

with

$$\vec{J}_T(k, t) = \sum_{j=1}^N \{\vec{v}_j(t) - [\vec{v}_j(t) \cdot \hat{k}]\hat{k}\} e^{i\vec{k} \cdot \vec{r}_j(t)} \quad (2)$$

for the transverse part, and

$$\vec{J}_L(k, t) = \sum_{j=1}^N \{[\vec{v}_j(t) \cdot \hat{k}]\hat{k}\} e^{i\vec{k} \cdot \vec{r}_j(t)} \quad (3)$$

for the longitudinal part. Here, $\vec{v}_j(t)$ is the velocity of particle j at time t , $k = |\vec{k}|$, and $\hat{k} = \vec{k}/|\vec{k}|$ with \vec{k} the wave vector.

Ideally, $C_\lambda(k, t)$ could usually be fitted by a function, $\exp(-\Gamma_\lambda t/2) \cos(\omega_\lambda t)$, where we could get the characteristic frequency ω_λ and the sound attenuation coefficient Γ_λ . However, recent studies [16,18,29] suggest that finite-size effects could prevent the fitting function from working in the long-time tail of $C_\lambda(k, t)$ in a finite-size system. Therefore, we follow the restricted envelope fit method [16,29] to eliminate the finite-size effects in the calculation of sound attenuation.

An illustration of using the restricted envelope fit method is shown in Fig. 1. Figure 1(a) shows a typical transverse current correlation function $C_T(k, t)$ in 2D glasses studied in this work. We determine the envelope $E_T(k, t)$ corresponding to $C_T(k, t)$ as peak values in $|C_T(k, t)|$, the absolute value of the $C_T(k, t)$; see Fig. 1(b). We then fit in Fig. 1(c), $E_T(k, t)$ to $\exp(-\Gamma_T t/2)$. One could observe that the fitting can no longer work when the time exceeds a characteristic timescale, which is denoted as $t_{c,\lambda}$. We checked the dependence of $t_{c,\lambda}$ on other parameters in Fig. 6 in the Appendix, and found that $t_{c,\lambda}$ depends on, e.g., the wave vector and the polarization, but varies little with temperatures for a fixed wave vector. As explained in previous studies [16,18,29], the deviation of $C_T(k, t)$ from the fitting function at time larger than t_c is due to finite-size effects. Hence, we get Γ_T by fitting $E_T(k, t)$ up to around t_c ; see Fig. 1(c). A more detailed discussion with respect to the finite-size effects on sound attenuation can be found in Refs. [16,18,29].

Moreover, to ensure the reliability of our methods used in this work, we show in Fig. 7 in the Appendix the comparison of the sound attenuation and disperse relation in glasses at a very low temperature and at zero temperature. The sound attenuation and frequency in the very low-temperature glasses are obtained from the fit to the current density correlation function [see Eq. (1)], while those in the zero-temperature glasses are from the fit to the velocity correlation function calculated during the integration of a harmonic equation of motion; see Refs. [16,19,20] for more details. One would expect that the two methods could produce the same results in the zero- and finite-temperature glasses, provided that the

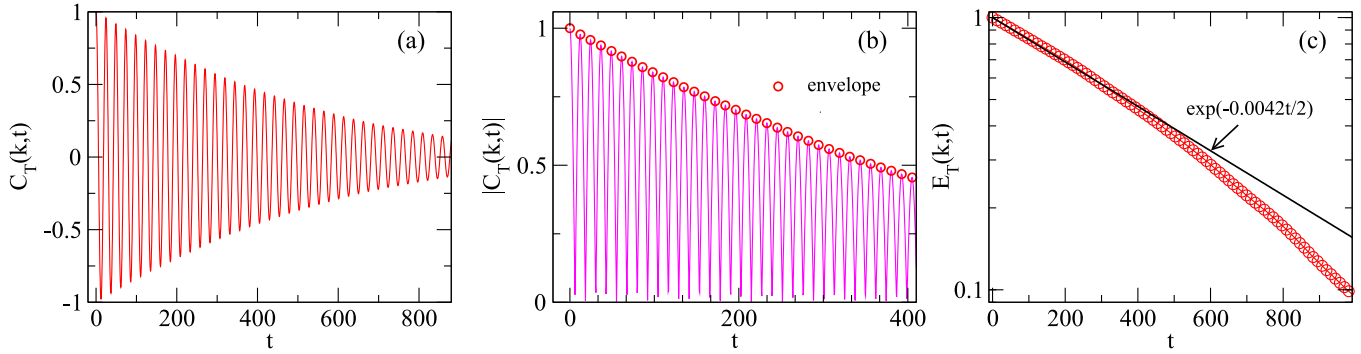


FIG. 1. An illustration showing how we obtain the sound attenuation coefficient Γ using the restricted envelope fit method. (a) The time evolution t of the transverse current correlation function $C_T(k, t)$ at a wave vector $k \approx 0.089$. (b) The absolute value of $C_T(k, t)$, $|C_T(k, t)|$ and (c) the corresponding envelope $E_T(k, t)$. In (b), we define the envelope as the peaks of $|C_T(k, t)|$. For visualization purposes, we do not show in (b) all the data corresponding to that shown in (a). The solid line in (c) indicates $E_T(k, t) = \exp(-\Gamma_T t/2)$ with $\Gamma_T \approx 0.0042$. We get Γ_T by the fit to $E_T(k, t)$ in the short-time regime, where $E_T(k, t)$ does not deviate from the fitting line; we note that the fail of the fit at longer time is due to finite-size effects, as explained in detail in Refs. [16,18,29].

temperature for the finite-temperature glasses is so low that anharmonic effects could be neglected. Our comparison suggests that the two methods could indeed lead to consistent results.

III. RESULTS AND DISCUSSION

A. Waiting time dependence of sound attenuation in poorly annealed glasses

Our finite-temperature glass could be characterized by three parameters, i.e., temperature T , parent temperature T_p , and the waiting time t_w . These parameters couple together to determine the stability of the resulting glass. We first study how t_w affects sound attenuation with both T_p and T fixed. Since t_w refers to how long the glass is annealed before our production run, it is expected a larger t_w will result in a more stable glass. For our very stable low-temperature glasses with, e.g., $T_p = 0.03$, we observe no visible dependence of sound attenuation on t_w within our simulation time window. We note here that our t_w that is examined is up to one million. However, for our very poorly annealed glasses, we do find t_w could have a marked influence on sound attenuation, which will be discussed in this section.

We show the waiting time t_w dependence of the transverse sound attenuation $\Gamma_T(k)$ in Fig. 2(a) and longitudinal sound attenuation $\Gamma_L(k)$ in Fig. 2(b), respectively, in our very poorly annealed glasses with ($T = 0.03$, $T_p = 0.40$). For the transverse part, we find that $t_w = 100$ and $t_w = 1$ M will result in two glasses with the same sound attenuation at large k , suggesting that the high- k sound attenuation does not depend on the examined waiting times. However, the resulting two glasses with $t_w = 100$ and $t_w = 1$ M exhibit markedly different scalings of sound attenuation at very small k . For instance, one could observe $\Gamma_T(k) \sim k^{1.5}$ in the $t_w = 100$ glass, but $\Gamma_T(k) \sim k^2$ in the $t_w = 1$ M glass. We find the same scenario in which the waiting time only affects the low- k sound attenuation also applies to the longitudinal part; see Fig. 2(b). In addition, for $t_w = 100$, we could observe the $k^{1.5}$ scaling of $\Gamma_T(k)$ spans a wider wave-vector range than that of $\Gamma_L(k)$. We note that if one wants to observe a more obvious distinction

of the low- k longitudinal sound attenuations in glasses with, e.g., $t_w = 100$ and $t_w = 1$ M, a much larger system than the one that we are examining in this work is needed.

The influence of waiting time on sound attenuation in the poorly annealed 2D glasses examined here resembles that in 3D glasses observed in Ref. [29]. Specifically, it has been reported in Ref. [29] that the low- k scaling of sound attenuation changes from $k^{1.5}$ to k^2 with increasing waiting time in 3D poorly annealed glasses with the same potential model in this work. However, we notice that the study [27,28] of poorly annealed monodisperse Leonard-Jones 3D glasses suggests that $\Gamma \sim k^{1.5}$ at small wave vector, and it remains unknown whether increasing the waiting time in these glasses could reach a different scaling. Therefore, we conclude that the non-negligible influence of waiting time on the low-wave-vector sound attenuation in poorly annealed glasses could be generalized to different dimensions, at least in the glasses examined in our model.

B. Temperature dependence of sound attenuation and its related properties in stable glasses

As mentioned in the previous section, our glasses' stability is controlled by a combination of T_p , T , and t_w . Our

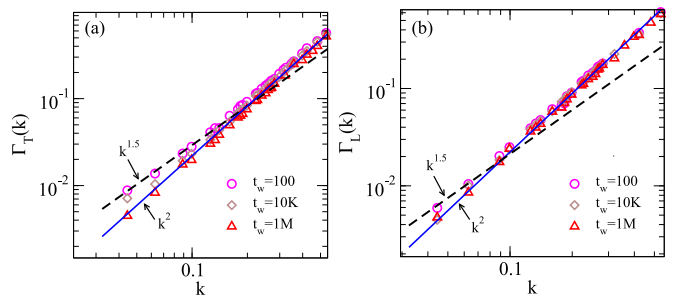


FIG. 2. Waiting time t_w dependence of sound attenuation for (a) transverse modes and (b) longitudinal modes in very poorly annealed glasses ($T = 0.03$, $T_p = 0.40$). The scaling of $\Gamma_T(k)$ with k changes from around $k^{1.5}$ to k^2 , with t_w increased from $t_w = 100$ to $t_w = 1$ M, as does the scaling of $\Gamma_L(k)$.

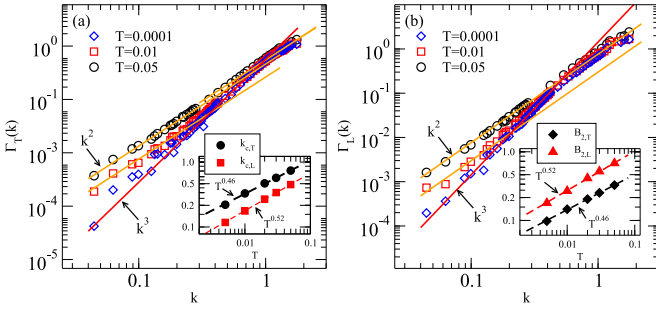


FIG. 3. Temperature T dependence of the (a) transverse and (b) longitudinal sound attenuation in very stable glasses with ($T_p = 0.03$, $t_w = 100$). We find that the change of t_w over a wide time range from $t_w = 10$ to $t_w = 1$ M does not alter the sound attenuation in these low-temperature stable glasses examined here. The inset in (a) shows the correlation between $k_{c,\lambda}$ and T . $k_{c,\lambda}$ at each T is defined as the wave vector at the intersection of two lines: One line represents the low- k scaling, $\Gamma_\lambda(k) \sim k^2$, and the other one represents the intermediate- k Rayleigh scattering scaling, $\Gamma_\lambda(k) \sim k^3$. The inset in (b) shows the temperature dependence of the quadratic coefficient $B_{2,\lambda}$ in $\Gamma_\lambda(k) = B_{2,\lambda}k^2$ at very low k . The black and red dashed lines in the insets correspond to power laws of $T^{0.46}$ and $T^{0.52}$, respectively. We find $k_{c,T} \sim B_{2,T} \sim T^{0.46}$ while $k_{c,L} \sim B_{2,L} \sim T^{0.52}$.

calculation shows that sound attenuation in our very stable glasses does not show visible change with the t_w that we have examined. However, we find that the sound attenuation in the stable glasses is sensitive to T when the anharmonicity induced by thermal motions becomes not negligible. We discuss in Fig. 3 how T affects sound attenuation in our most stable glasses with $T_p = 0.03$ and $t_w = 100$.

For the transverse part in Fig. 3(a) and longitudinal part in Fig. 3(b), the Rayleigh scattering scaling $\Gamma_\lambda(k) \sim k^3$ seems to work well without interruption in the low- k regime at $T = 0.0001$. Note that we find $\Gamma_\lambda(k)$ at $T = 0.0001$ and $T = 0$ is almost the same; see Fig. 7 in the Appendix. With increasing T , the influence of anharmonic effects on sound attenuation becomes visible within our probed wave-vector regime. For glasses at $T = 0.01$ and $T = 0.05$, we can observe $\Gamma_\lambda(k) = B_{2,\lambda}k^2$ at small $k \leq k_{c,\lambda}$, and both $B_{2,\lambda}$ and $k_{c,\lambda}$ increase with increasing T for $\lambda = T$ (or $\lambda = L$). It should be noted that we observe no $k^{1.5}$ scaling of $\Gamma_\lambda(k)$ in these stable glasses at all the examined waiting times, which is markedly different than the case in poorly annealed 2D glasses as shown in Fig. 2.

At the very large- k regime, there is a nearly T -independent quadratic scaling of $\Gamma_\lambda(k)$, which is different from the low- k quadratic scaling that depends on T . With increasing T , the low- k and high- k quadratic scalings of $\Gamma_\lambda(k)$ have the trend to merge. In between the low- k and high- k quadratic scaling regimes is the Rayleigh scattering scaling, $\Gamma_\lambda(k) \sim k^3$, whose prefactor, i.e., $\Gamma_\lambda(k)/k^3$, does not depend on T . However, the Rayleigh scattering scaling regime contracts with increasing T and nearly disappears at very high T . Therefore, we conclude that the temperature-induced anharmonicity affects sound attenuation more at low k than at intermediate k , but it has nearly no effects on the high- k sound attenuation. This is qualitatively similar to what have been reported when studying the T dependence of sound attenuations in 3D stable glasses [29].

We next studied in a more quantitative way how T changes the upper wave-vector limit $k_{c,\lambda}$ for the low- k scaling of $\Gamma_\lambda(k) = B_{2,\lambda}k^2$; we also checked how T changes the quadratic coefficient $B_{2,\lambda}$. The T dependence of $k_{c,T}$ and $k_{c,L}$ is shown in the inset to Fig. 3(a), while in the inset to Fig. 3(b) is the T dependence of $B_{2,T}$ and $B_{2,L}$. We determine, e.g., $k_{c,T}$ as the intersection of the low- k quadratic and the intermediate- k cubic power-law fitting lines. One can observe that $k_{c,\lambda}$ becomes larger with increasing T , suggesting the influence of stronger anharmonicity induced by increasing T extends to a larger k . Our tentative fitting suggests that $k_{c,\lambda} \sim T^\gamma$ with $\gamma \approx 0.46$ for $\lambda = T$, but $\gamma \approx 0.52$ for $\lambda = L$. For the quadratic coefficient $B_{2,\lambda}$, it also goes up with increasing T , and hence the low- k sound modes in a higher-temperature glass are scattered more. At a fixed T , we find $B_{2,L}$ is always larger than $B_{2,T}$. This suggests that for modes with the same wavelength, the longitudinal modes are scattered more severely than the transverse ones. In addition, we find the fits of the $B_{2,\lambda}$ vs T data to power laws, $B_{2,L} \sim T^{0.46}$ and $B_{2,L} \sim T^{0.52}$, could work well. Hence, the above analysis in 2D stable glasses suggests that $k_{c,T} \sim B_{2,T} \sim T^{0.46}$, while $k_{c,L} \sim B_{2,L} \sim T^{0.52}$. It has been reported [29], in 3D stable glasses with the same potential model as employed in this work, that $B_{2,T} \sim T^{0.48}$. We notice how $B_{2,L}$ scales with T was not given explicitly in Ref. [29]. Therefore, the way $B_{2,T}$ depends on T in 2D stable glasses is very similar to that in 3D glasses. It should be noted here that we used power laws which could fit our data well, but we do not exclude that other fitting functions may also work.

Recent simulations have suggested that the longitudinal sound attenuation is proportional to the transverse one when plotted as a function of frequency ω in 3D glasses at zero temperature [16,17] and finite temperatures [29], i.e., $\Gamma_T(\omega) = S * \Gamma_L(\omega)$, with S a scaling constant. The existence of such a linear correlation could simplify the study of sound attenuation. Specifically, one sometimes does not have to calculate both parts: Longitudinal and transverse sound attenuation; instead, one only needs to calculate one part and then get the other one by extrapolation from the linear relation. This is more important to experimental studies of sound attenuation because the longitudinal sound attenuation can be obtained directly from scattering experiments, while it is technically difficult to perform a direct measurement of the transverse sound attenuation in realistic experiments [22–25]. Here, the linear relation $\Gamma_T(\omega) = S * \Gamma_L(\omega)$ is tested numerically in 2D glasses though it has proven to be valid in 3D glasses by simulations.

We show in Fig. 4 the sound attenuation as a function of frequency ω in our 2D stable glasses, which are the same glasses examined in Fig. 3. One can observe that the relation $\Gamma_T(\omega) = S * \Gamma_L(\omega)$ is still valid at different T . At intermediate temperatures, e.g., at $T = 0.01$, $\Gamma_\lambda(\omega)$ scales with ω squared at low and high ω , and the Rayleigh scattering scaling works at intermediate ω . However, we find that the scaling constant S exhibits a non-negligible dependence on T , e.g., we find S changes by about 20% when T varies from 0.0001 to 0.05. This is different from the finding that S is nearly independent of T in 3D stable glasses [29]. We note that we find $\Gamma_T(\omega) \sim \Gamma_L(\omega)$ could also work in our poorly annealed 2D glasses.

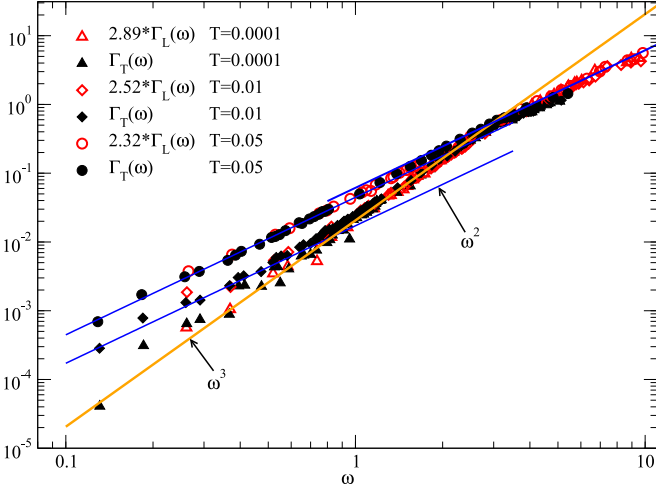


FIG. 4. Sound attenuation as a function of frequency in stable glasses with the same $T_p = 0.03$ and $t_w = 100$, but different T . The glasses examined here are the same as shown in Fig. 3, where sound attenuation is plotted as a function of the wave vector. $\Gamma_L(\omega)$ at each T is scaled by a factor S to achieve the best collapse between $\Gamma_L(\omega)$ and $\Gamma_T(\omega)$. We find that S exhibits a non-negligible temperature dependence, e.g., $S \approx 2.89$ for $T = 0.0001$, $S \approx 2.52$ for $T = 0.01$, and $S \approx 2.32$ for $T = 0.05$.

In the last part of this section, we move on to study how the anharmonicity induced by temperatures affects sound ve-

locities; the related results are reported in Fig. 5. Note that the glasses examined in Fig. 5 have the same $T_p = 0.03$ as those examined in Figs. 3 and 4. We first compare the disperse relation for transverse excitations $\omega_T(k)$ in Fig. 5(a) and longitudinal excitations $\omega_L(k)$ in Fig. 5(b) at $T = 0.0001$, $T = 0.01$, and $T = 0.05$. One could observe that there is almost no visible difference in $\omega_T(k)$ or $\omega_L(k)$ between the three finite-temperature glasses. However, as shown in Fig. 3, the same three glasses exhibit an obvious difference in the low- k behaviors of both $\Gamma_T(k)$ and $\Gamma_L(k)$. Therefore, it appears that the anharmonicity affects the sound attenuation more than the disperse relation. Moreover, $\omega_\lambda(k)$ seems to scale linearly with k in the $\omega_\lambda(k)$ vs k representation, whereas it has been suggested that $C_\lambda(k) = \omega_\lambda(k)/k$ is not always a constant in the $C_\lambda(k)$ vs k representation. We find it to be the case; see Fig. 5(c) for the transverse polarization and Fig. 5(d) for the longitudinal one. $C_T(k)$ shows a minimum at around a wave vector k_m , in agreement with previous results [16,17,19,20,27,37–39]. In particular, above k_m , $C_T(k)$ increases with increasing k , which is usually referred to as sound hardening, while below k_m , $C_T(k)$ increases with decreasing k , which is referred to as sound softening. Note that at the lowest wave vectors that we examined, $C_T(k)$ is approaching a plateau. The data in Fig. 5(d) for $C_L(k)$ follow a similar scenario, except that the hardening of longitudinal sound is not obvious in our probed range of k .

Since both $C_L(k)$ and $C_T(k)$ appear to be a plateau at the lowest wave vectors in each finite-temperature glass,

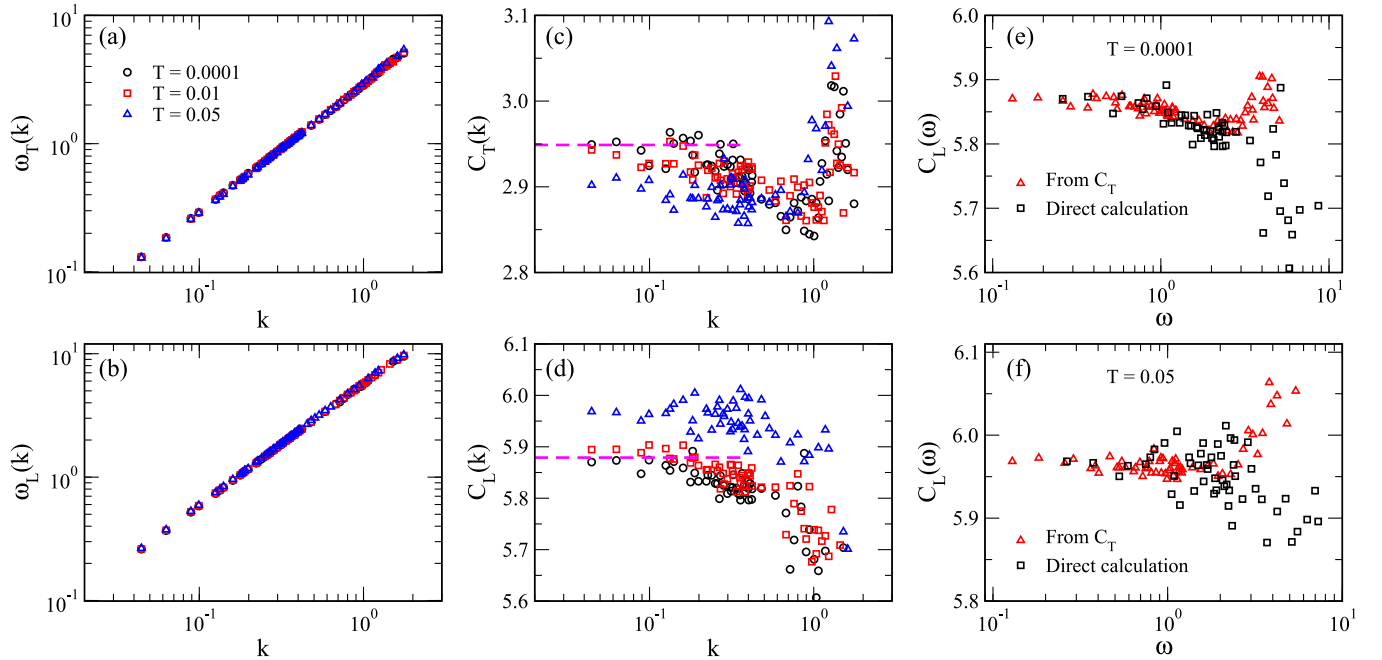


FIG. 5. Temperature dependence of (a), (b) frequency $\omega_\lambda(k)$ and (c), (d) sound velocity $C_\lambda(k) = \omega_\lambda(k)/k$ for glasses with the same $T_p = 0.03$ and $t_w = 100$. The horizontal dashed lines in (c) and (d) indicate the macroscopic values of the transverse and longitudinal sound velocities, $C_T(0)$ and $C_L(0)$, in $T = 0$ glasses. $C_T(0)$ and $C_L(0)$ were calculated from the shear modulus G and bulk modulus B as follows: $C_T(0) = \sqrt{G/\rho}$ and $C_L(0) = \sqrt{(G+B)/\rho}$. Note that we obtained G and B in $T = 0$ glasses by performing quasistatic deformation simulations; for reference, $G \approx 8.70$ and $B \approx 25.87$ in $T = 0$ glasses. In (e) and (f), the longitudinal sound velocity $C_L(\omega)$ calculated from $C_L(\omega) = \omega_L/k$ is compared with $C_L(\omega)$ calculated from the corresponding transverse sound velocity, i.e., $C_L(\omega) = \sqrt{B/\rho + C_T^2(\omega)}$. Following Refs. [17,19], we assume here that B is frequency independent. B in our finite-temperature glasses is derived from the macroscopic sound velocities which are determined from the low- k plateau in $C_\lambda(k)$ vs k plots.

we check to see whether the values of $C_T(k)$ and $C_L(k)$ at the lowest wave vectors are around their corresponding macroscopic values in the long-wavelength limit, $C_T(0)$ and $C_L(0)$. We obtained $C_T(0)$ and $C_L(0)$ in 2D glasses as follows: $C_T(0) = \sqrt{G/\rho}$ and $C_L(0) = \sqrt{(G+B)/\rho}$, with G the shear modulus and B the bulk modulus. In Fig. 7 in the Appendix, we could see no difference in $\omega_\lambda(k)$ between $T = 0.0001$ and $T = 0$ glasses, and the two glasses also have nearly the same $\Gamma_\lambda(k)$. Therefore, we assume the anharmonicity due to thermal motions in $T = 0.0001$ glasses could be negligible. In line with this reasoning, we use $C_\lambda(0)$ calculated at $T = 0$ to represent $C_\lambda(0)$ in $T = 0.0001$ glass. Note that it has been suggested in simulation studies [17,19] that the low- k plateau value of $C_\lambda(k)$ coincides with the corresponding macroscopic $C_\lambda(0)$. Taking these together, we would expect $C_\lambda(0)$ obtained at $T = 0$ could be approximately equal to the height of the low- k plateau of $C_\lambda(k)$ at $T = 0.0001$. We find it to be the case. Specifically, the dashed lines indicating $C_T(0)$ from $T = 0$ glasses in Fig. 5(c) and $C_L(0)$ from $T = 0$ glasses in Fig. 5(d) could go through the low- k data for $C_T(k)$ and $C_L(k)$ in $T = 0.0001$ glasses, respectively. Note that the dashed lines in Figs. 5(c) and 5(d) are also close to the low- k $C_\lambda(k)$ data for $T = 0.01$ glasses.

Next, we check how the macroscopic moduli change with the anharmonicity. We first obtained the macroscopic values $C_\lambda(0)$ in each finite-temperature glass from the low- k plateau of $C_\lambda(k)$, and then extracted the corresponding B and G from $C_\lambda(0)$. As a result, we find $G \approx 8.70$ at $T = 0.0001$, 8.66 at $T = 0.01$, and 8.42 at $T = 0.05$, while $B \approx 25.76$ at $T = 0.0001$, 26.08 at $T = 0.01$, and 27.20 at $T = 0.05$. Hence, G decreases, though mildly, with increasing temperature, which is expected since the glasses become less stable with increasing temperatures; however, the corresponding B increases systematically, though also mildly, with increasing temperature, which is not expected. We notice that the unexpected decrease of bulk modulus with increasing glass stability has even been reported in Ref. [8], where the authors studied the same model glasses as examined in this work but in 3D and at $T = 0$, and the glass stability is tuned by parent temperatures from which $T = 0$ glasses are quenched. In addition, we find B decreases as well with increasing glass stability (or decreasing T_p) in zero-temperature 2D glasses, e.g., B changes approximately from 32.44 to 25.87 with T_p decreased from 0.40 to 0.03. Further work is needed to understand the decrease of bulk modulus with increasing glass stability.

Moreover, it was suggested in Ref. [17] by studying Leonard-Jones glasses that the simple proportionality between the frequency dependence of the longitudinal and transverse sound attenuations, $\Gamma_L(\omega)$ and $\Gamma_T(\omega)$, is accompanied by a simple relation between the longitudinal and transverse sound velocities, i.e., $C_L(\omega) = \sqrt{B/\rho + C_T^2(\omega)}$ in 2D and $C_L(\omega) = \sqrt{B/\rho + \frac{4}{3}C_T^2(\omega)}$ in 3D, where B is assumed to be frequency independent and equal to its macroscopic value. This simple relation was found to work as well in glasses with a purely repulsive harmonic potential [19]. However, we also notice that it was reported in Ref. [39] that the pro-

posed simple relation may not be general. Since we could observe the proportionality between $\Gamma_T(\omega)$ and $\Gamma_L(\omega)$ in different finite-temperature glasses (see Fig. 4), it would be interesting to check whether the previously proposed simple relation between the longitudinal and transverse sound velocities could work in our 2D glasses. We compare in Figs. 5(e) and 5(f) the $C_L(\omega)$ data obtained by the fit to the current density correlation function and the $C_L(\omega)$ data derived from $C_T(\omega)$ by assuming B is a constant. We find that the simple relation between the longitudinal and transverse sound velocities could work over a wide range of frequencies in our examined 2D glasses, though there seems to be a deviation from the relation in the very high-frequency regime.

IV. CONCLUSION

In this work, we studied numerically how the anharmonicity induced by thermal motions alters sound attenuation in finite-temperature 2D glasses. We focused on two kinds of glasses with markedly different stabilities: One is very poorly annealed glass with small stability, and the other one is very stable glass whose stability is comparable to that of experimental glass. The stability of our studied glasses is determined by the parent temperature T_p , temperature T , and waiting time t_w . We find that the anharmonicity affects mainly the transverse and longitudinal sound attenuation in the low-wave-vector regime in all the examined glasses, irrespective of the glass stability; however, the way it affects sound attenuation depends on the glass stability. Specifically, the anharmonicity makes finite-temperature glasses feature a very low-wave-vector regime where $\Gamma_\lambda \sim k^\beta$ with $\beta \neq 3$, which is absent in zero-temperature glasses within the harmonic approximation. In our very poorly annealed glasses at finite temperature, the scaling exponent β depends on t_w , i.e., β is around 1.5 for short t_w , but converges to around 2.0 with the increase of t_w . However, in our very stable glasses, we observe $\beta \approx 2.0$, independent of t_w throughout our largest available simulation time window. Moreover, we studied the T dependence of the low-wave-vector quadratic scaling of $\Gamma_\lambda(k) = B_{2,\lambda}k^2$ in stable glasses. We find the upper wave-vector limit $k_{c,\lambda}$ for this quadratic scaling increases with T , and so does the quadratic coefficient $B_{2,\lambda}$. To be more quantitative, we find $k_{c,T} \sim B_{2,T} \sim T^{0.46}$ while $k_{c,L} \sim B_{2,L} \sim T^{0.52}$. This suggests that increasing anharmonicity not only extends the low-wave-vector quadratic scaling regime, but also enhances the amplitude of the sound attenuation at the same wave vector. In addition, in our examined 2D stable glasses, when plotted as a function of frequency, the longitudinal sound attenuation is linearly proportional to the corresponding transverse one; the longitudinal sound velocity could be derived from the corresponding transverse one by simply assuming a frequency-independent bulk modulus. Hence, taken together with previous investigations in 3D glasses [29], we conclude that the way the anharmonicity affects sound attenuation does not depend on the spatial dimension.

We note that the nonquadratic scaling of sound attenuation with wave vectors has been predicted by the fluctuating

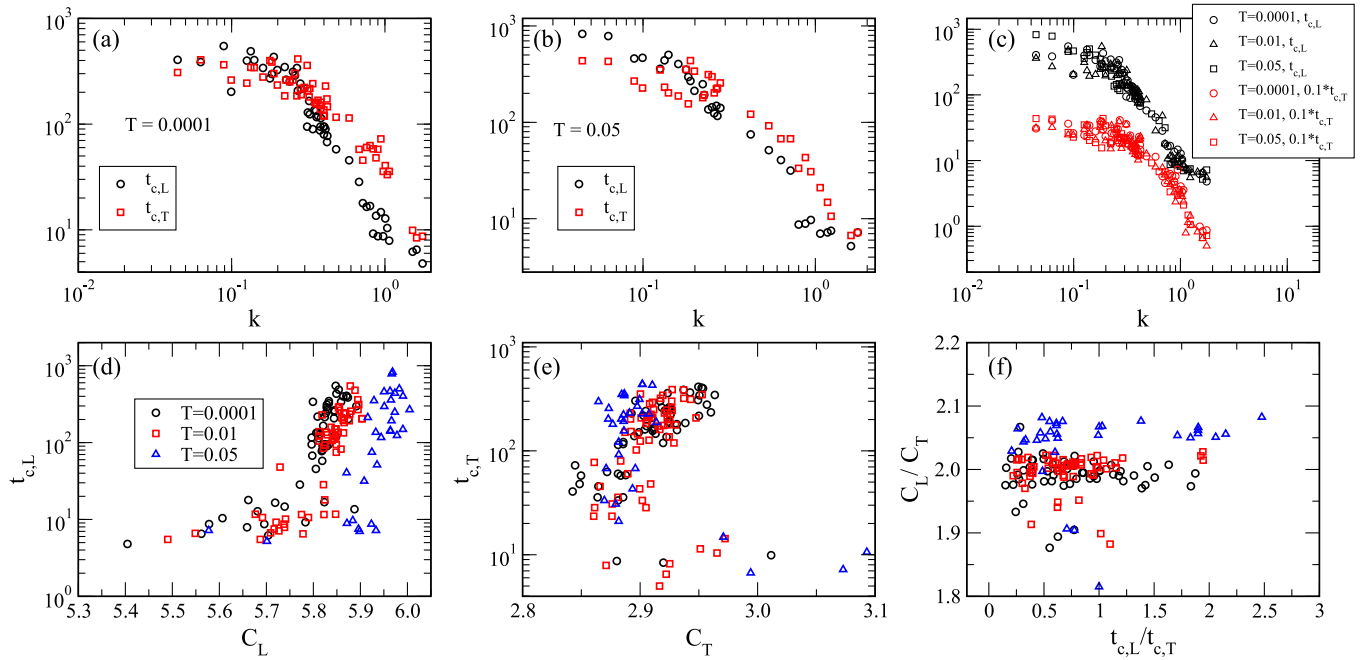


FIG. 6. Comparison of the characteristic time $t_{c,T}(k)$ and $t_{c,L}(k)$ in (a) $T = 0.0001$ and (b) $T = 0.05$ glasses. The characteristic time $t_{c,\lambda}(k)$ refers to the time above which the fit of the exponential decay to the envelope fails; see Fig. 1(c). For glasses at a fixed temperature, one could observe that $t_{c,T}(k)$ and $t_{c,L}(k)$ show a small difference at very small k , but exhibit a systematic but small difference at larger k . In addition, both $t_{c,T}(k)$ and $t_{c,L}(k)$ approximately exhibit a very low- k plateau, and then decrease monotonically with increasing k . (c) Temperature dependence of $t_{c,T}(k)$ and $t_{c,L}(k)$ which has been scaled by a factor of 0.1 for visualization purposes. One could observe that both $t_{c,T}(k)$ and $t_{c,L}(k)$ are nearly independent of the examined temperatures. For additional reference, we plot (d) $t_{c,L}(k)$ vs $C_L(k)$, (e) $t_{c,T}(k)$ vs $C_T(k)$, and (f) $C_L(k)/C_T(k)$ vs $t_{c,L}(k)/t_{c,T}(k)$. The symbols in (d)–(f) have the same meanings. Note that glasses at $T = 0.0001$, $T = 0.01$, and $T = 0.05$ have the same $T_p = 0.03$ and $t_w = 100$.

elasticity theory [11,26,30], i.e., the anharmonicity results in a nonquadratic scaling of sound attenuation in glasses with marginal elastic instability. Moreover, it is worth noting that this theory is an equilibrium theory which assumes a heterogeneous elasticity in space. However, in our simulation studies of poorly annealed glasses, we observe that the nonquadratic scaling appears when the waiting time is short, but disappears when the waiting time is long enough. Therefore, the nonquadratic scaling seems to be a nonequilibrium transient phenomena from our simulation study. Further work is needed to reconcile this inconsistency between the simulation and theory.

Recent studies [16,18,31] show that within the harmonic approximation in both 2D and 3D glasses, the sound attenuation correlates well with the density of excess modes, $D(\omega)$, beyond the Debye prediction. Therefore, it would be interesting to check whether the correlation persists at finite temperatures, which needs to figure out how $D(\omega)$ changes with ω when taking into account anharmonicity. Very recently, it has been suggested that the frequency ω dependence of $D(\omega)$ relies on the spatial dimension in the harmonic approximation [31]. Specifically, for excess modes hybridizing with phonon modes in large-scale glasses, $D(\omega) \sim \omega^4$ in 3D glasses, while $D(\omega) \sim \omega^2$ in 2D glasses, when $D(\omega)$ is determined by subtracting off the Debye contribution from the total density of states. We notice that studies of 3D small glasses [40,41] at finite temperatures suggested that

$D(\omega) \sim \omega^4$ below the first sound mode. However, how $D(\omega)$ scales with ω at very low frequencies below the first sound mode remains a matter of debate, even in the harmonic approximation, in both 3D and 2D glasses [31,42,43]. This hinders one from further claiming which changes in the scaling of $D(\omega)$ in finite-temperature glasses result from the anharmonicity. Moreover, it remains unknown how $D(\omega)$ changes with ω at finite temperatures in very large glasses whose low-frequency excess modes may be in the frequency regime where the anharmonicity could affect sound attenuation. Further work is needed to examine the scaling of $D(\omega)$ with ω in these finite-temperature glasses, in particular, to check whether the effect of anharmonicity on the ω dependence of $D(\omega)$ relies on the spatial dimension.

ACKNOWLEDGMENTS

We thank A. Ninarello for generously providing equilibrated configurations at very low parent temperatures. We acknowledge the support from National Natural Science Foundation of China (Grant No. 12004001), Anhui Projects (Grants No. S020218016 and No. Z010118169), Hefei City (Grant No. Z020132009), and Anhui University (start-up fund). We also acknowledge the Hefei Advanced Computing Center, Beijing Super Cloud Computing Center, and the High-Performance Computing Platform of Anhui University for providing computing resources.

APPENDIX: SUPPORTING FIGURES

In this Appendix, we show further results in Figs. 6 and 7 to support some of our descriptions in the main text.

We show how the characteristic time t_c changes with wave vectors in Figs. 6(a)–6(c), and sound velocities in Figs. 6(d) and 6(e) in finite-temperature glasses. Note that the characteristic time t_c refers to the time above which the fit of the exponential decay to the envelope fails; see Fig. 1(c). We find that t_c is almost a constant at our lowest wave vectors and decreases with increasing wave vectors; t_c seems to depend on the polarization (transverse or longitudinal) for the same wave vector, but depends little on temperatures for the same wave vector and polarization; see Fig. 6(c). In addition, we show in Fig. 6(f) the ratio of the longitudinal sound velocity to the transverse one vs the ratio of the longitudinal characteristic time to the transverse one. The ratio of sound velocities is almost a constant if ignoring several fluctuating points, while the ratio of the characteristic timescales could change from around 0.25 to 2.0.

In Fig. 7, we compared sound attenuation and dispersion relation in very low-temperature and zero-temperature glasses. We expect that glasses at a low enough temperature and glasses at zero temperature should show no difference in, e.g., disperse relation and sound attenuation. For the very low-temperature glasses, we got the sound attenuation and frequency from the fit to the current density correlation functions [see Eq. (1)], while for zero-temperature glasses, we got the sound attenuation and frequency through the fit to velocity correlation functions calculated during the integration of an equation of motion within the harmonic approximation; see Ref. [16] for more details. We find that the two different methods could lead to consistent results, which could help further ensure the reliability of our results.

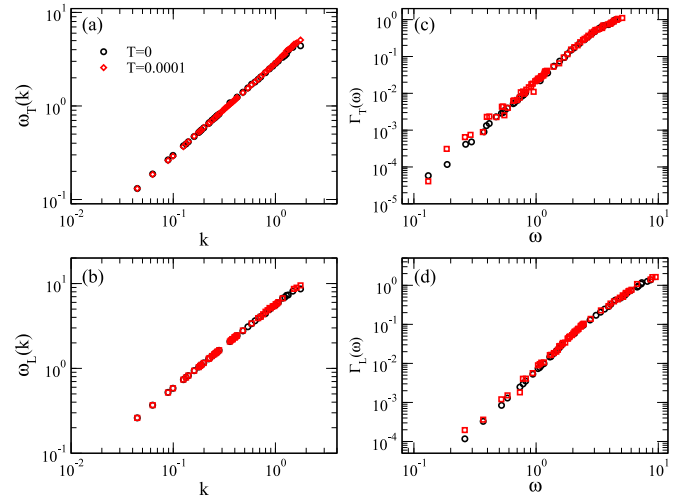


FIG. 7. Comparison of sound attenuation results in $T = 0$ and $T = 0.0001$ glasses with the same $T_p = 0.03$. (a) The transverse frequency $\omega_T(k)$ and (b) the longitudinal one $\omega_L(k)$; (c) the transverse sound attenuation coefficient $\Gamma_T(\omega)$ and (d) the longitudinal one $\Gamma_L(\omega)$. For $T = 0.0001$ glasses, we got sound attenuation coefficient and frequency from the current density correlation functions [see Eq. (1)], while we got those in $T = 0$ glasses using a different method, i.e., through the fit to velocity correlation functions calculated during the integration of an equation of motion within the harmonic approximation; see Refs. [16,19,20] for more details regarding this method. Symbols in (a)–(d) have the same meanings. One would expect that the anharmonicity induced by thermal motions is negligible at low enough temperatures. The examined temperature $T = 0.0001$ turns out to be low enough not to induce anharmonicity, since $\omega_\lambda(k)$ at $T = 0.0001$ and $T = 0$ shows almost no difference, as does $\Gamma_\lambda(\omega)$. Therefore, our two different methods used to extract sound attenuation information could lead to consistent results.

- [1] L. Berthier and G. Biroli, *Rev. Mod. Phys.* **83**, 587 (2011).
- [2] H. Zong, H. Wu, X. Tao, D. Xue, J. Sun, S. J. Pennycook, T. Min, Z. Zhang, and X. Ding, *Phys. Rev. Lett.* **123**, 015701 (2019).
- [3] R. C. Zeller and R. O. Pohl, *Phys. Rev. B* **4**, 2029 (1971).
- [4] R. O. Pohl, X. Liu, and E. Thompson, *Rev. Mod. Phys.* **74**, 991 (2002).
- [5] M. P. Zaitlin and A. C. Anderson, *Phys. Rev. B* **12**, 4475 (1975).
- [6] E. Lerner, G. During, and E. Bouchbinder, *Phys. Rev. Lett.* **117**, 035501 (2016).
- [7] H. Mizuno, H. Shiba, and A. Ikeda, *Proc. Natl. Acad. Sci. USA* **114**, E9767 (2017).
- [8] L. Wang, A. Ninarello, P. Guan, L. Berthier, G. Szamel, and E. Flenner, *Nat. Commun.* **10**, 26 (2019).
- [9] E. Flenner, L. Wang, and G. Szamel, *Soft Matter* **16**, 775 (2020).
- [10] W. Schirmacher, G. Ruocco, and T. Scopigno, *Phys. Rev. Lett.* **98**, 025501 (2007).
- [11] C. Tomaras, B. Schmid, and W. Schirmacher, *Phys. Rev. B* **81**, 104206 (2010).
- [12] E. DeGiuli, A. Laversanne-Finot, G. Düring, E. Lerner, and M. Wyart, *Soft Matter* **10**, 5628 (2014).
- [13] G. Szamel and E. Flenner, *J. Chem. Phys.* **156**, 144502 (2022).
- [14] M. Baggioli and A. Zaccone, *J. Phys.: Condens. Matter* **34**, 215401 (2022).
- [15] C. Caroli and A. Lemaitre, *Phys. Rev. Lett.* **123**, 055501 (2019).
- [16] L. Wang, L. Berthier, E. Flenner, P. Guan, and G. Szamel, *Soft Matter* **15**, 7018 (2019).
- [17] G. Monaco and S. Mossa, *Proc. Natl. Acad. Sci. USA* **106**, 16907 (2009).
- [18] A. Moriel, G. Kapteijns, C. Rainone, J. Zylberg, E. Lerner, and E. Bouchbinder, *J. Chem. Phys.* **151**, 104503 (2019).
- [19] H. Mizuno and A. Ikeda, *Phys. Rev. E* **98**, 062612 (2018).
- [20] S. Gelin, H. Tanaka, and A. Lemaitre, *Nat. Mater.* **15**, 1177 (2016).
- [21] T. Scopigno, J. B. Suck, R. Angelini, F. Albergamo, and G. Ruocco, *Phys. Rev. Lett.* **96**, 135501 (2006).
- [22] G. Baldi, V. M. Giordano, B. Ruta, R. DalMaschio, A. Fontana, and G. Monaco, *Phys. Rev. Lett.* **112**, 125502 (2014).
- [23] C. Masciovecchio, G. Baldi, S. Caponi, L. Comez, S. Di Fonzo, D. Fioretto, A. Fontana, A. Gessini, S. C. Santucci, F. Sette,

- G. Viliani, P. Vilmercati, and G. Ruocco, *Phys. Rev. Lett.* **97**, 035501 (2006).
- [24] P. Benassi, S. Caponi, R. Eramo, A. Fontana, A. Giugni, M. Nardone, M. Sampoli, and G. Viliani, *Phys. Rev. B* **71**, 172201 (2005).
- [25] A. Devos, M. Foret, S. Ayrinhac, P. Emery, and B. Ruffle, *Phys. Rev. B* **77**, 100201(R) (2008).
- [26] C. Ferrante, E. Pontecorvo, G. Cerullo, A. Chiasera, G. Ruocco, W. Schirmacher, and T. Scopigno, *Nat. Commun.* **4**, 1793 (2013).
- [27] H. Mizuno and S. Mossa, *Condens. Matter Phys.* **22**, 43604 (2019).
- [28] H. Mizuno, G. Ruocco, and S. Mossa, *Phys. Rev. B* **101**, 174206 (2020).
- [29] L. Wang, G. Szamel, and E. Flenner, *Soft Matter* **16**, 7165 (2020).
- [30] A. Marruzzo, S. Köhler, A. Fratolocchi, G. Ruocco, and W. Schirmacher, *Eur. Phys. J.: Spec. Top.* **216**, 83 (2013).
- [31] L. Wang, G. Szamel, and E. Flenner, *Phys. Rev. Lett.* **127**, 248001 (2021); **129**, 019901(E) (2022).
- [32] E. Flenner and G. Szamel, *Nat. Commun.* **6**, 7392 (2015).
- [33] L. Berthier, P. Charbonneau, A. Ninarello, M. Ozawa, and S. Yaida, *Nat. Commun.* **10**, 1508 (2019).
- [34] A. Ninarello, L. Berthier, and D. Coslovich, *Phys. Rev. X* **7**, 021039 (2017).
- [35] S. Plimpton, *J. Comput. Phys.* **117**, 1 (1995).
- [36] <http://lammps.sandia.gov/>
- [37] Y. Wang, L. Hong, Y. Wang, W. Schirmacher, and J. Zhang, *Phys. Rev. B* **98**, 174207 (2018).
- [38] G. Monaco and V. M. Giordano, *Proc. Natl. Acad. Sci. USA* **106**, 3659 (2009).
- [39] H. Mizuno, S. Mossa, and J.-L. Barrat, *Proc. Natl. Acad. Sci. USA* **111**, 11949 (2014).
- [40] R. Guerra, S. Bonfanti, I. Procaccia, and S. Zapperi, *Phys. Rev. E* **105**, 054104 (2022).
- [41] P. Das and I. Procaccia, *Phys. Rev. Lett.* **126**, 085502 (2021).
- [42] F. C. Mocanu, L. Berthier, S. Ciarella, D. Khomenko, D. R. Reichman, C. Scalliet, and F. Zamponi, [arXiv:2209.09579](https://arxiv.org/abs/2209.09579).
- [43] L. Wang, L. Fu, and Y. Nie, *J. Chem. Phys.* **157**, 074502 (2022).